

A climatology of stratopause temperature and height in the polar vortex and anticyclones

J. A. France,^{1,2} V. L. Harvey,¹ C. E. Randall,^{1,2} M. H. Hitchman,³ and M. J. Schwartz⁴

Received 22 September 2011; revised 3 February 2012; accepted 7 February 2012; published 30 March 2012.

[1] A global climatology of stratopause temperature and height is shown using 7 years of Microwave Limb Sounder satellite data, from 2004 to 2011. Stratopause temperature and height is interpreted in the context of the polar vortices and anticyclones defined by the Goddard Earth Observing System meteorological analyses. Multiyear, monthly mean geographic patterns in stratopause temperature and height are shown to depend on the location of the polar vortices and anticyclones. The anomalous winters of 2005/2006 and 2008/2009 are considered separately in this analysis. In the anomalous years, we show that the elevated stratopause in February is confined to the vortex core. This is the first study to show that the stratopause is, on average, 20 K colder and 5–10 km lower in the Aleutian anticyclone than in ambient air during the Arctic winter. During September in the Antarctic the stratopause is, on average, 10 K colder inside anticyclones south of Australia. The regional temperature and height anomalies, which are due to vertical ageostrophic motion associated with baroclinic instability, are shown to be climatological features. The mean structure of the temperature and height anomalies is consistent with moderate baroclinic growth below the stratopause and decay above. This work furthers current understanding of the geography of the stratopause by emphasizing the role of synoptic baroclinic instability, whereby anticyclones establish zonally asymmetric climatological patterns in stratopause temperature and height. This work highlights the need to consider zonal asymmetries when calculating upper stratospheric temperature trends.

Citation: France, J. A., V. L. Harvey, C. E. Randall, M. H. Hitchman, and M. J. Schwartz (2012), A climatology of stratopause temperature and height in the polar vortex and anticyclones, *J. Geophys. Res.*, 117, D06116, doi:10.1029/2011JD016893.

1. Introduction

[2] Stratospheric temperature is a sensitive indicator of climate change because increasing concentrations of carbon dioxide (CO_2) act to cool the middle atmosphere [Rind *et al.*, 1998; *World Meteorological Organization*, 1998; Olivero and Thomas, 2001]. Ramaswamy *et al.* [2001] used lidar and rocket data to show that the upper stratospheric cooling trend of 1–2 K/decade increases with altitude, with the largest cooling of \sim 3 K/decade near the stratopause at 50 km between 1979 and 1999. It is therefore of interest to study the temperature at the stratopause, quantify natural variability, and understand mechanisms that modulate it. Different physical processes maintain the stratopause at different latitudes and seasons. At sunlit latitudes, the stratopause is characterized by a temperature maximum near 50 km due to the absorption of shortwave radiation by ozone. In the polar night there is no

solar insolation and a “separated” polar winter stratopause is maintained by gravity wave (GW) driven diabatic descent at high latitudes [e.g., Hitchman *et al.*, 1989]. During undisturbed conditions, the stratopause in the polar vortices is generally at higher altitudes and is warmer than in midlatitudes [e.g., Kanzawa, 1989]. However, when planetary wave amplitudes are large, such as during sudden stratospheric warming (SSW) events [Labitzke and Naujokat, 2000], the stratopause warms by up to 50 K between the vortex and the Aleutian anticyclone and descends more than 20 km inside the anticyclone over several days [e.g., Labitzke, 1977, 1981]. Recent results suggest that the frequency of major SSWs will increase in the 21st century [Charlton-Perez *et al.*, 2008].

[3] When planetary waves break, they form anticyclones that can extend from the upper troposphere to the middle mesosphere. Stratospheric anticyclones are ubiquitous features in the Arctic winter [e.g., Harvey and Hitchman, 1996; Harvey *et al.*, 2002] and Antarctic spring [e.g., Mechoso *et al.*, 1991]. Thus while the temperature and height of the stratopause in the vortex are maintained by GW-driven descent, planetary waves and anticyclones dominate high-latitude variability. Waugh and Randel [1999] presented a climatology of the polar vortices up to \sim 40 km altitude, which describes interannual variability and compares the two hemispheres. This paper presents the first climatology of the geographic distribution of stratopause temperature and

¹Laboratory for Atmospheric and Space Physics, University of Colorado at Boulder, Boulder, Colorado, USA.

²Department of Atmospheric and Oceanic Sciences, University of Colorado at Boulder, Boulder, Colorado, USA.

³Atmospheric and Oceanic Sciences Department, University of Wisconsin-Madison, Madison, Wisconsin, USA.

⁴Jet Propulsion Laboratory, Pasadena, California, USA.

height interpreted with respect to the location of the polar vortices and anticyclones. A clear relationship of the synoptic evolution of stratopause anomalies with polar vortices and anticyclones locations is demonstrated.

[4] An outline of this paper is as follows. Section 2 describes the meteorological analyses and satellite data used in this work. Section 3 outlines the analysis methods used to define the stratopause, polar vortices, and anticyclones. Section 4 shows the 7-year mean annual cycle of zonal mean stratopause temperature and height as a function of latitude and time. Section 5 discusses geographic patterns in stratopause height and temperature, both with a case study in the 2008 Arctic winter and with monthly mean results in both hemispheres. It also discusses the relationship of the wintertime season-average stratopause to polar vortices and anticyclones. Section 6 presents time series that illustrate the interannual variability of stratopause temperature and height in the polar vortices and anticyclones in both hemispheres. Conclusions are given in section 7.

2. Meteorological Analyses and Satellite Data

2.1. Goddard Earth Observing System Model

[5] The Goddard Earth Observing System (GEOS) model version 5 uses an Atmospheric General Circulation Model (AGCM) and the Grid Point Statistical Interpolation to generate the Data Assimilation System. The dynamics that are integrated into the GEOS AGCM are from the Earth System Modeling Framework [Rienecker et al., 2007]. The model integrates 6 h observational data with a 6 h general circulation model using an Incremental Analysis Updating process, which uses the assimilated data to create a constant forcing on the GCM over 6 h intervals. This is different from nudging, which is a one-time force applied when the data is assimilated [Bloom et al., 1996]. A complete list of observations that are assimilated into the model is given by Rienecker et al. [2007, Table 3.5.1]. GEOS uses two GW parameterizations: drag from orographic GWs based on the work of McFarlane [1987] and drag from nonorographic GWs based on the work of Garcia and Boville [1994]. These are tuned to yield a realistic stratosphere and mesosphere in the free-running model [Pawson et al., 2008]. For this analysis, GEOS version 5.1 is used prior to 1 September 2008, after which we use GEOS version 5.2.

[6] Pressure, temperature, geopotential height, and horizontal winds are provided every 6 h at 72 equally spaced vertical levels from 1 km to 72 km on a 0.5° latitude by $2/3^\circ$ longitude grid. In this work, daily averaged products are linearly interpolated to a 2.5° latitude by 3.75° longitude grid and to potential temperature levels ranging from 300 K (~ 10 km) to 5000 K (~ 80 km). The potential temperature levels chosen correspond to a vertical resolution of ~ 2 km in the upper stratosphere and lower mesosphere. The algorithm used to demarcate the polar vortices and anticyclones is an extension of the method described by Harvey et al. [2002], which accounts for circumpolar anticyclones. We interpolate this “vortex marker” field to the height of the stratopause.

2.2. Microwave Limb Sounder

[7] The Microwave Limb Sounder (MLS) instrument is on NASA’s Aura satellite, which was launched on 15 July 2004 into a 705 km Sun-synchronous orbit [Waters et al., 2006].

MLS samples every 165 km along the satellite track. Each day ~ 3500 vertical profiles are available up to a latitude of 82° in each hemisphere. MLS measures thermal microwave emissions from the Earth’s limb. Temperature is inferred from emission of oxygen at 118 GHz. Version 3 temperature data are used in this work [Livesey et al., 2011]. The vertical resolution of the temperature measurements is ~ 5.5 km at ~ 3 hPa and ~ 8 km at 0.01 hPa. At the stratopause, the temperature precision is ~ 1 K and there is a ~ 1 K cold bias, as inferred from coincident comparisons with eight correlative data sets [Schwartz et al., 2008; Livesey et al., 2011]. GEOS version 5.2 analyses are used as a priori information in the retrieval of MLS temperature. Uncertainties due to noise and a priori information range from 0.6 K in the stratosphere to 2.5 K in the mesosphere. Temperature data are filtered using version 3 status, quality, and convergence values provided by the MLS science team [Livesey et al., 2011].

[8] For this work, we focus on the evolution of stratopause temperature and height patterns at middle-to-high latitudes. Thus our analysis requires year-round global coverage. While the Sounding of the Atmosphere using Broadband Emission Radiometry (SABER) instrument provides temperature measurements with better vertical resolution (~ 3 km) at the stratopause [Mertens et al., 2001] compared to MLS, the yaw of the SABER instrument results in data void regions poleward of 52° latitude for half of the year in both hemispheres [Russell et al., 1999]. Therefore the results shown here are based entirely on MLS data. Since SABER temperature profiles have higher vertical resolution near the stratopause, we reproduced the stratopause climatology using SABER and compared it to MLS in regions and times where instrument sampling overlapped. Despite differences in local time sampling between MLS and SABER, monthly mean stratopause temperature and height differences are within ~ 2 K and ~ 2 km, respectively. Since these differences between MLS and SABER are smaller than the geographical differences in the stratopause in the vortex and anticyclones (described below), we conclude that the vertical resolution of MLS is sufficient for our analysis.

[9] Following the major SSWs of 2006 and 2009, the stratopause in the Arctic vortex reformed within a week at an altitude of ~ 80 km and the upper stratospheric vortex strengthened [e.g., Hauchecorne et al., 2007; Siskind et al., 2007; Manney et al., 2008a, 2008b, 2009, and references therein]. Because the 2006 and 2009 elevated stratopause events occurred within the timeframe of this climatology, and these events result in an anomalously high Arctic stratopause in February and March of 2006 and 2009, we consider these periods separately in our analysis.

3. Analysis Methods

[10] In this work, GEOS data are used to demarcate the polar vortices and anticyclones while MLS temperatures are used to define the temperature and height of the stratopause. On each day we construct a horizontal grid of MLS temperature on the GEOS longitude-latitude grid. The grid consists of one day of observations and is created by applying a spatial Delaunay Triangulation at each vertical level. A distance weighted smoothing process is applied to the gridded data to ensure differentiability. Finally, we interpolate from pressure

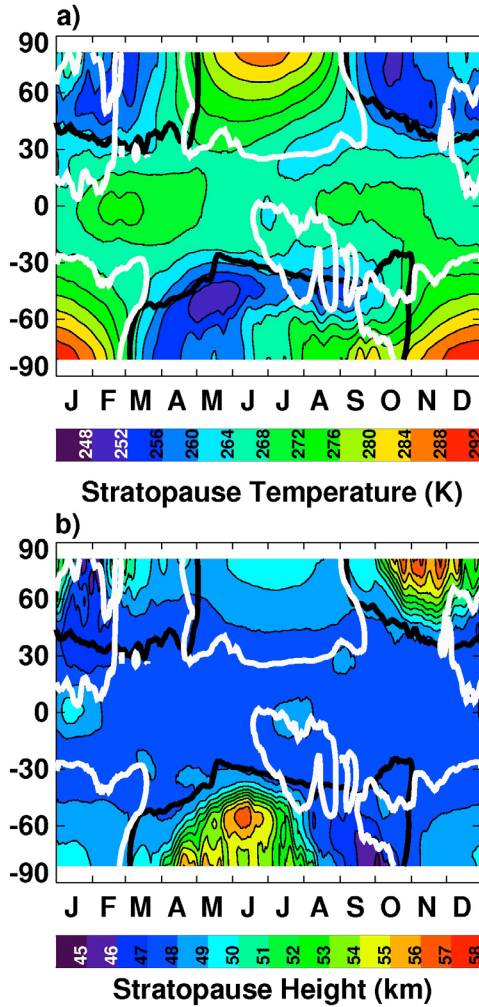


Figure 1. The 7-year average annual cycle of stratopause (a) temperature and (b) height as a function of latitude based on MLS data from August 2004 through July 2011. Thick black and white contours indicate 5% of the maximum frequency of occurrence of the vortex and anticyclones, respectively, based on GEOS. February and March of 2006 and 2009 are not included. Tick marks on the horizontal axis denote the 1st of each month.

to geometric altitude from 10 km to 120 km at 1 km increments.

[11] The stratopause is typically characterized by a temperature maximum in the middle atmosphere. Like the tropopause, the stratopause has been traditionally viewed as a single two-dimensional layer. In general, this conceptual model is sufficient, but it is not adequate in all situations. In particular, it does not discriminate when there are multiple local temperature maxima in a single vertical profile. Multiple local temperature maxima occur when there are Mesospheric Inversion Layers (MILs) [i.e., *Meriwether and Gerrard*, 2004], SSWs, deep isothermal layers, and noise in the temperature profiles. It is difficult to demarcate the “true” stratopause in these situations.

[12] For this work, the following procedure is used to define the stratopause for each vertical temperature profile.

An 11 km boxcar smoothing is applied to each temperature profile from which a temperature maximum (Tmax) is identified between 20 km and 85 km. In order to proceed, the lapse rate must be negative (positive) at the five adjacent 1 km increment levels above (below) Tmax. If this condition is satisfied then the altitude of Tmax in the smoothed profile is used as a central altitude to search ± 15 km for Tmax in the unsmoothed profile. The temperature and altitude of Tmax in the unsmoothed profile is then demarcated as the stratopause. If the conditions above are not satisfied, no stratopause is defined in the temperature profile.

[13] At middle-high latitudes, the frequency of multiple temperature maxima ranges from 2% to 11% of the profiles depending on longitude and season. At low latitudes the frequency is close to zero. Removing temperature profiles with more than one local maximum has only a small effect on the climatology, changing the average stratopause temperature by less than 1 K and stratopause height by less than 1 km. A thorough analysis of multiple stratopause events is the subject of future work.

4. Latitude-Time Evolution of the Stratopause

[14] Figure 1 shows the 7-year average annual cycle of stratopause temperature (Figure 1a) and height (Figure 1b) as a function of latitude. Each day of the year is a 7-year average zonal mean using MLS data from August 2004 through July 2011. February and March of 2006 and 2009 are not included in Figure 1 because the stratopause was at anomalously high altitudes during these months; as discussed more below, this led to significant differences poleward of 30° N between these years and the others in February and March. A 7-day running mean is applied at each latitude to emphasize seasonal variability. Thick black and white contours indicate 5% of the maximum frequency of occurrence of the vortex and anticyclones, respectively, based on GEOS.

[15] Notable features in the stratopause temperature (Figure 1a) include the warm polar summer stratopause in both hemispheres; the cold stratopause at the edge of the polar vortices in midwinter, consistent with *Barnett* [1974] and *Labitzke* [1974]; and the tropical semiannual oscillation, consistent with *Hood* [1986] and *Hitchman and Leovy* [1986]. Since low latitudes are always sunlit for at least part of each day, seasonal temperature changes are significantly smaller (± 5 K) than at higher latitudes (± 35 K). The cold winter polar vortex is interrupted in midwinter by warming over the pole due to GW-driven subsidence from the mesosphere [Kanzawa, 1989; *Hitchman et al.*, 1989; *Garcia and Boville*, 1994; *Duck et al.*, 2001]. This warm anomaly is less coherent in the boreal winter due to midwinter SSWs and mesospheric coolings in the Northern Hemisphere (NH) [e.g., *Labitzke*, 1981].

[16] In both hemispheres, the summer anticyclones occur poleward of $\sim 30^{\circ}$ latitude, where the stratopause is 20–30 K warmer than in the winter polar night. There is a significant difference in stratopause anticyclone occurrence between the two hemispheres during winter, where late winter and spring anticyclones occur between 30° N and 60° N but between 20° S and 40° S, reflecting the ability of the stronger austral vortex to keep anticyclones from penetrating to higher latitudes.

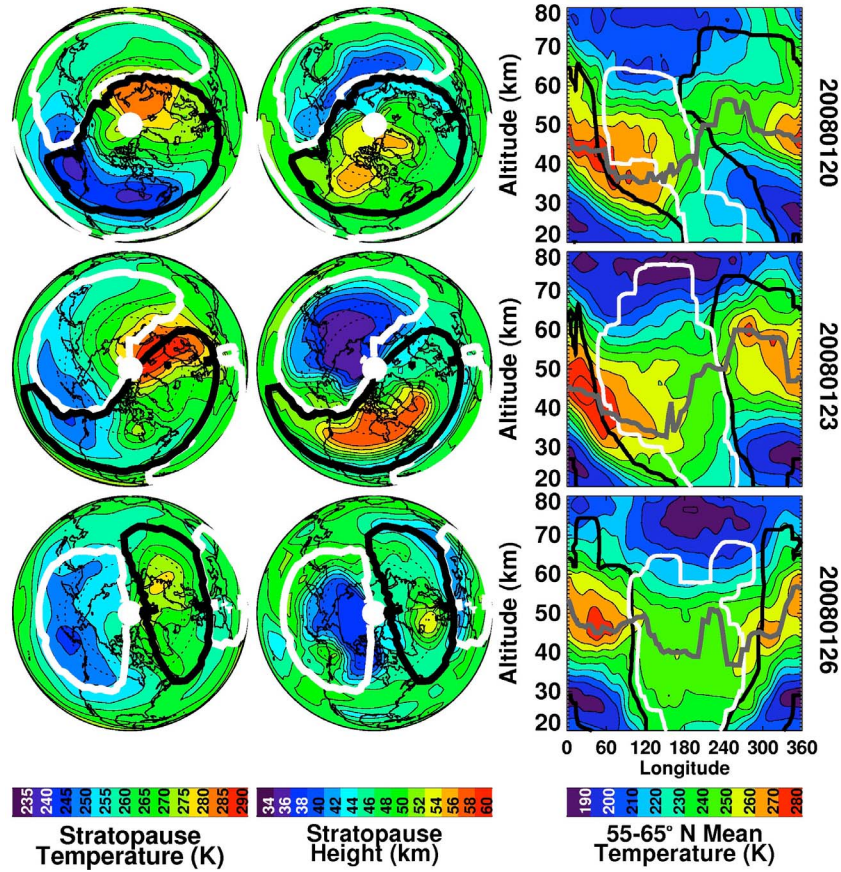


Figure 2. Polar orthographic projections of (left) stratopause temperature, (middle) stratopause height, and (right) longitude-altitude plots of temperature averaged between 55°N and 65°N for a case study in the NH for 20, 23, and 26 January 2008. The Greenwich Meridian is oriented to the right. The polar vortex (anticyclone) edge, based on GEOS data, is indicated by the thick black (white) contours. The thick gray contour indicates the stratopause height.

[17] Figure 1b shows that in the NH, the polar stratopause altitude inside the vortex increases toward the winter solstice due to the lower solar zenith angle and increased altitude of maximum solar heating. Planetary wave driven mesospheric cooling events help lower the polar stratopause during boreal winter (DJF) and austral spring, along with the return of the Sun to higher zenith angles. In general, the climatological zonal mean stratopause temperature and stratopause altitude appear to be anticorrelated. Subsidence can lower and warm the stratopause, while ascent can raise and cool the stratopause. However, we will find that the zonal mean temperature and height of the stratopause do not show a complete picture of their relationship and zonal asymmetries must be considered to understand the correlation between stratopause temperature and height.

5. Geographic Patterns in Stratopause Temperature and Height

[18] A primary aspect underlying the climatological results is the role of synoptic weather events during which deep, tilted anticyclones move poleward and eastward around the Arctic [e.g., Harvey *et al.*, 2002] and Antarctic [e.g., Mechoso *et al.*, 1991; Farrara *et al.*, 1992; Lahoz *et al.*, 1996] polar vortices. These events are responsible

for anomalies in multiyear, monthly mean distributions of stratopause temperature and height in the NH winter. These events are also observed in the Southern Hemisphere (SH), but the amplitude of the stratopause temperature and height anomalies is not as large, and the anticyclones move much faster. Thus while there are distinct cases where cold and low stratopause anomalies follow SH anticyclones, their effects on multiyear monthly mean stratopause anomalies are not as apparent as in the NH. Here we show a representative case study in the NH to illustrate the daily evolution of the stratopause, polar vortices, and anticyclones during such events. This is followed by a multiyear, monthly mean climatology of stratopause temperature and height anomalies and the mean geographic locations of the polar vortices and anticyclones at the stratopause in both hemispheres. In the Arctic, a separate 2-year “climatology” is shown for the anomalous years of 2005/2006 and 2008/2009.

5.1. Case Study: January 2008

[19] Figure 2 shows a case study in the NH that illustrates the daily evolution of the Arctic vortex, anticyclones, and stratopause on 3 days in which stratopause temperature and height anomalies are associated with the location of the polar vortex and anticyclones. MLS stratopause temperature

(height) is shown in the left (center) column, similar to what is shown by *Manney et al.* [2008a, Figure 8]. The polar vortex and anticyclone edge, based on GEOS data, are indicated by the thick black and white contours, respectively. At the stratopause, temperature anomalies are out of phase with respect to height anomalies. This can be understood in terms of westward tilt with height and hydrostatic thicknesses, as seen in longitude-altitude sections. The right column shows the vertical temperature structure averaged between 55° N and 65° N latitude. In the longitude-altitude sections the stratopause is indicated by a thick gray contour, and the polar vortex and anticyclones are depicted as in the polar maps. The geographic patterns in stratopause temperature and height during this case study are in very good agreement with SABER; temperature and height differences are less than 2 K and 2 km, respectively (not shown).

[20] On 20 January 2008 (top row) there is a large anticyclone that extends from ~50°E to 170°E longitude and 30°N to 60°N latitude. The Arctic vortex is displaced from the pole and is roughly centered over Greenland. The warm and cold anomalies in stratopause temperature are offset by ~90° from the circulation systems; both the highest and lowest stratopause temperatures are located near the vortex edge, with the region of highest stratopause temperatures (~280 K) lying near the boundary between the Arctic vortex and the anticyclone over Siberia. The lowest temperatures (~240 K) occur to the east of the anticyclone near the vortex edge over the North Pacific and United States-Canadian border. The stratopause is at highest altitudes inside the polar vortex over North America and Greenland and at lowest altitudes along the poleward flank of the anticyclone. The longitude-altitude section shows the anticyclone and vortex are tilted westward with height. The stratopause is warmest and lowest between the eastern edge of the vortex and the western edge of the anticyclone. Conversely, the stratopause is coldest and highest between the western edge of the vortex and the eastern edge of the anticyclone. This is a classic example of a stratospheric baroclinic system described by *Thayer et al.* [2010]. In the mesosphere, there is a cold pool above the anticyclone and the warm anomaly located to the east of the vortex in the stratosphere extends up to 80 km.

[21] This baroclinic system is particularly well defined on 23 January 2008 (middle row). By this date the anticyclone has moved poleward and eastward and has expanded so that it covers nearly 180° of longitude and from 30° N to the pole. The vortex is distorted on this day; the anticyclone-vortex pair is indicative of planetary wave breaking. Stratopause height anomalies are in quadrature with the temperature anomalies; the maximum and minimum temperature anomalies are between the vortex and the anticyclone while the height extremes are located inside the circulation systems. There are large horizontal gradients in both the temperature and height of the stratopause over the pole. Stratopause temperature decreases more than 40 K from the Eastern Arctic Ocean to the North Pacific and the stratopause height slopes downward 20 km from Canada to Russia. These structures are similar to front-like structures shown by *Fairlie et al.* [1990]. The orthogonal relationship between the temperature anomalies and the circulation systems indicates that there is cold and warm air advection and vertical ageostrophic motion associated with planetary wave growth due to

baroclinic instability [*Thayer et al.*, 2010]. On this day a second anticyclone develops over the subtropical Atlantic Ocean. While there is not a stratopause temperature anomaly associated with this anticyclone, the height of the stratopause is ~5 km lower between this second anticyclone and the polar vortex. The longitude-altitude plot shows that the vortex and anticyclones tilt westward with height (though not as severely as on 20 January), another indication that ageostrophic vertical motions associated with baroclinic instability drive the temperature anomalies. The stratopause is below 35 km inside the anticyclone and near 60 km in the vortex. As on 20 January, there are low temperatures along the eastern edge of the anticyclones due to local ascent and high temperatures along the western edge of the anticyclones due to local descent. This plot indicates low temperatures inside the anticyclone at 70 km compared to temperatures inside the vortex. The opposite is true at 30 km.

[22] On 26 January 2008 (bottom row) the stratopause temperature and height anomalies are both collocated with the high-latitude circulation systems. Inside the Aleutian anticyclone, stratopause temperatures are low (245 K to 250 K) compared to inside the polar vortex (270 K to 280 K). The stratopause inside the second anticyclone (now over the Mediterranean Sea) is ~5 K colder and ~8 km lower than at other longitudes at the same latitude. The air inside this second anticyclone originated from lower latitudes and the lower, cooler stratopause reflects this origin. It is also possible that the tropical air inside the anticyclone cools radiatively and sinks, contributing to the lower stratopause. This anticyclone continues to move poleward and eastward and has similar stratopause temperature and height anomalies as shown on 23 January (not shown). The longitude-altitude area indicates that the vortex and Aleutian anticyclone are vertically stacked, and westward tilting temperature anomalies are no longer evident. This is an indication that the system is barotropic and in its decaying phase [e.g., *Holton*, 2004]. In the stratosphere, the temperature structure indicates large vertical gradients inside the vortex, while inside the anticyclone the atmosphere is nearly isothermal. Note that the coldest mesospheric longitudes lie over the anticyclone, shifting eastward with time as the anticyclone becomes more barotropic. The cold mesosphere above the anticyclone (compared to other longitudes) is the subject of future work.

5.2. Monthly Mean Polar Maps of the Stratopause

[23] Here we show the evolution of multiyear monthly mean stratopause temperatures and heights during the months in which the polar vortices are present at the stratopause in each hemisphere. The vortex is well established from October through March in the NH and from April through October in the SH [e.g., *Harvey et al.*, 2002, Figure 11].

5.2.1. Northern Hemisphere Typical Seasons

[24] In the Arctic, a 5-year climatology is shown for years in which the stratopause was not anomalously elevated. An additional 2-year “climatology” follows for the anomalous 2005/2006 and 2008/2009 seasons. Figure 3 shows NH polar projections of 5-year monthly mean stratopause temperature (left column) and height (right column) for the months in which the Arctic vortex is present in 2004/2005,

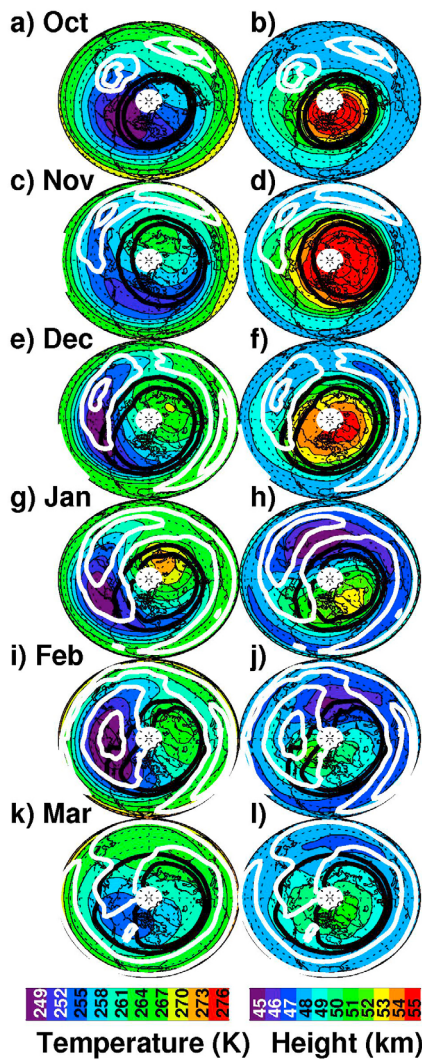


Figure 3. NH polar orthographic projections of monthly mean stratopause (left) temperature and (right) height. Seasons included are 2004/2005, 2006/2007, 2007/2008, 2009/2010, 2010/2011. The Greenwich Meridian is oriented to the right. Months from October through March are shown. Thick black vortex (white anticyclone) contours represent 50% and 70% (30% and 70%) of the maximum frequency of occurrence value at each grid point for a given month. In March the anticyclone contour is 10%.

2006/2007, 2007/2008, 2009/2010, and 2010/2011. Thick black (white) contours indicate locations where the polar vortex (anticyclones) occur. Vortex (anticyclone) contours represent 50% and 70% (30% and 70%) of the maximum frequency of occurrence value at each grid point for a given month. For March, the 10% anticyclone contour is shown. This lower contour emphasizes that, while infrequent, high-latitude anticyclones are observed in March. Locations where anticyclone and vortex contours overlap represent places where both anticyclones and the vortex occur at the same grid point but on different days of the month.

[25] The monthly evolution of the stratopause, the Arctic vortex, and NH anticyclones is as follows. During October, the stratopause in the vortex is coldest (Figure 3a) compared

to any other month of the year. The stratopause is \sim 10 km higher inside the vortex compared to latitudes equatorward of the vortex edge (Figure 3b). There are large horizontal gradients in stratopause height inside the vortex with the highest altitudes occurring in the vortex core. While the stratopause height maximum is near the center of the vortex, the stratopause is coldest at the edge of the vortex over Canada. In November, both warm and cold stratopause anomalies are located at the vortex edge (Figure 3c). Thus taking a zonal average (even in equivalent latitude space) would obscure zonal asymmetries that are common in the NH. It is interesting to note that the cold anomaly over the Canadian Arctic is warmer in November than every other month except March. This is not well understood; we hypothesize that in November, there is more GW-driven descent than during October and less baroclinicity than in DJF. The stratopause is at highest altitudes (\sim 55 km) in November (Figure 3d) compared to all other months shown. The stratopause is elevated throughout the entire polar vortex, with large gradients in stratopause height near the edge of the vortex. During the autumn months, anticyclones are generally confined to the subtropics and do not correlate with anomalies in stratopause temperature or height.

[26] In December (Figures 3e and 3f), January (Figures 3g and 3h), and February (Figures 3i and 3j), planetary “wave 1” signatures dominate the stratopause temperature patterns. This is due to the climatological Aleutian anticyclone that is present over 60% of the time at 60° N and the Date Line [Harvey and Hitchman, 1996]. At this location, the stratopause temperature is \sim 20 K lower and the stratopause height is 5–10 km lower in the vicinity of the anticyclone compared to other longitudes. This can be understood in terms of the baroclinic structure of the planetary waves [Simmons, 1974]. In the stratosphere, temperature usually decreases poleward, so geostrophic flows around planetary wave ridges and troughs advect cold air equatorward to the west of a trough and warm air poleward to the east of the trough. From hydrostatic thickness arguments this implies a westward tilt with increasing altitude for the axes of height and temperature maxima. There is an important transition from a structure supporting baroclinic growth below the stratopause to baroclinic decay above the stratopause in the time mean. Near the stratopause, the vertical motion field associated with the baroclinic wave becomes a primary mechanism responsible for the offset between stratopause temperature and height anomalies in the climatological mean [Thayer et al., 2010].

[27] In March (Figures 3k and 3l), the vortex and anticyclones weaken and stratopause temperature is generally inversely correlated with stratopause height. The cold region centered over the Canadian Arctic is colocated with stratopause height maxima.

5.2.2. Northern Hemisphere Anomalous Seasons

[28] Figure 4 shows NH monthly mean polar projections for the two seasons in which the stratopause was anomalously elevated (2005/2006 and 2008/2009). In October, November, and December (Figures 4a–4f), this “climatology” is similar to Figure 3, although stratopause temperature in the cold pool over Western Canada and the North Pacific monotonically decreases.

[29] In January (Figures 4g and 4h), the stratopause is lower and colder over most of the hemisphere compared to

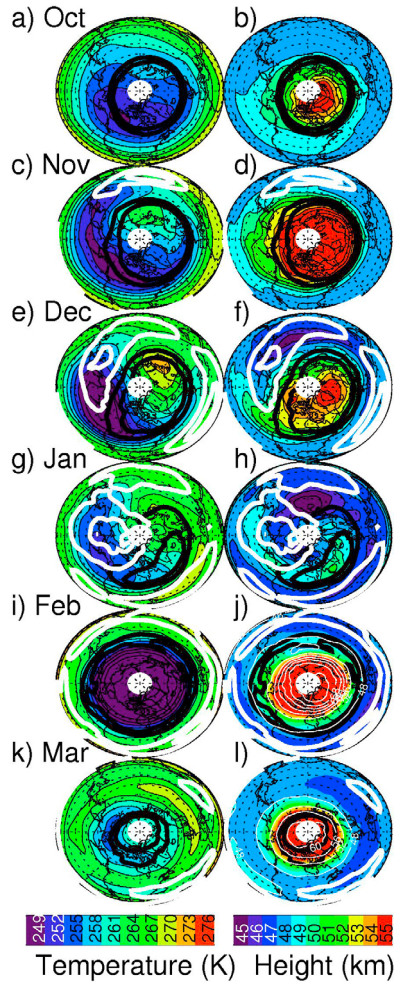


Figure 4. Same as Figure 3, but for the 2005/2006 and 2008/2009 seasons. For the stratopause height in February and March, thin white contours are plotted every 4 km.

Figures 3g and 3h. Compared to the 5-year climatology shown in Figure 3, dramatic differences in both the stratopause and the circulation are observed in February (Figures 4i and 4j). During this month, the stratopause is cold throughout a large zonally symmetric Arctic vortex but the elevated stratopause is confined to the vortex core. Stratopause height contours in February and March are white and spaced every 4 km. In February, there are large meridional gradients in stratopause height within the vortex (Figure 4j). The height of the stratopause in the vortex decreases from ~ 72 km at 80° N to ~ 53 km at 60° N and to ~ 48 km at 40° N (near the vortex edge). In March, only the height of the stratopause inside the vortex is drastically different from Figure 3l, with the highest value at 61 km poleward of 75° N.

5.2.3. Southern Hemisphere

[30] Figure 5 is the same as Figure 3, but for the SH months of April through October and using 7 years of data from 2004 and 2011. In general, inside the Antarctic vortex the stratopause warms continuously from April through October. The height of the stratopause in the vortex rises from April through June and then descends from June through October. To first order, the evolution of stratopause

temperature and height in the Antarctic vortex is due to GW-driven descent maximizing in the winter followed by ozone heating dominating in spring.

[31] The monthly evolution of the stratopause, the Antarctic vortex, and SH anticyclones is as follows. From April through June, stratopause temperatures are lowest at the edge of the Antarctic vortex (Figures 5a, 5c, and 5e), most likely because there is weak ozone heating and weak GW-driven descent. During these months, the height of the stratopause monotonically rises inside the vortex (Figures 5b, 5d, and 5f). In May, June, and to a lesser degree in July, there is a sharp gradient (~ 10 km over 5° in latitude) between the height of the stratopause inside versus outside the vortex (Figures 5d, 5f, and 5h). During these months, the relatively warm stratopause in the vortex is not pole centered; rather, the warmest region is displaced toward 45° E longitude (Figures 5c, 5e, and 5g). This zonal asymmetry may be due to the planetary wave train, excited by tropical convection over Indonesia, which modulates the Antarctic vortex [Hitchman and Rogal, 2010].

[32] In August, September, and October (Figures 5i through 5n), the stratopause in the vortex warms and descends. This is likely due to the return of sunlight to the polar

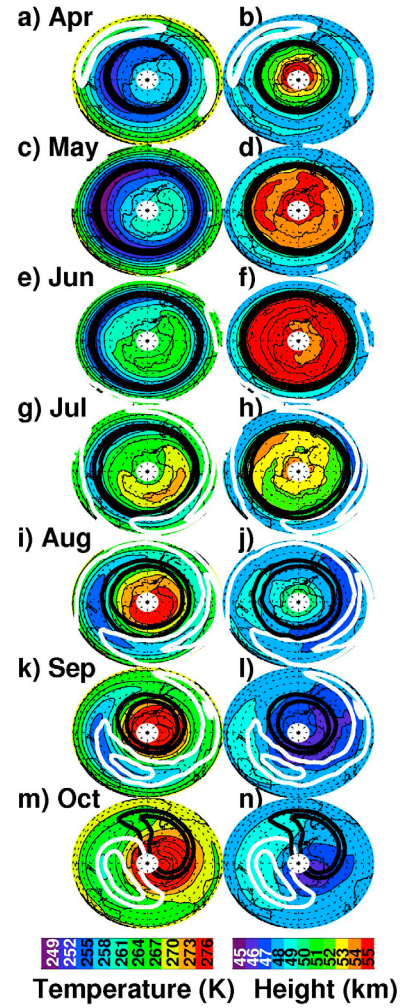


Figure 5. Same as Figure 3, but in the SH for the months of April through October. All years are included.

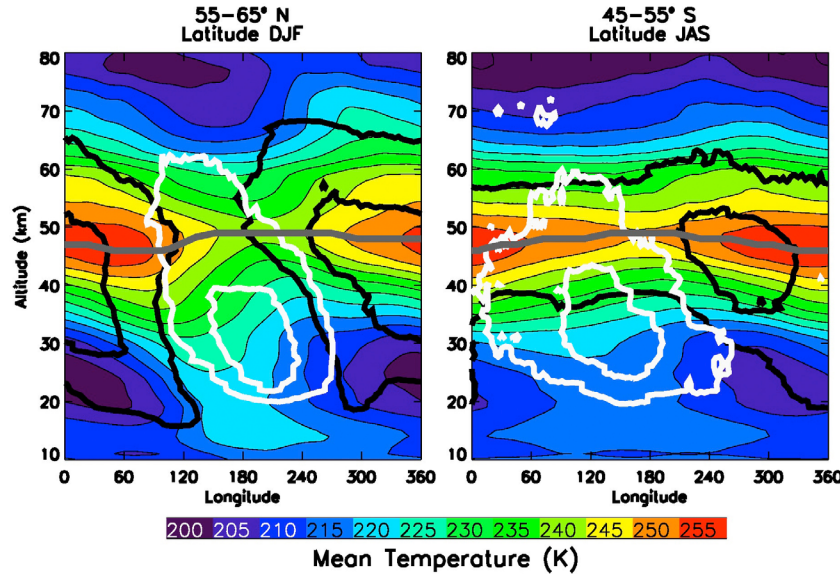


Figure 6. Longitude-altitude plots of MLS temperature averaged between (left) 55 and 65°N for DJF and (right) 45 and 55°S for JAS. The thick black, white, and gray contours represent the vortex, anticyclones, and stratopause, respectively.

regions, increased planetary wave amplitudes, decreased GW-driven descent in the mesosphere, and nonlinear wave-mean flow interactions [e.g., Matsuno, 1970; Hitchman *et al.*, 1989]. In September and October, anticyclones are observed between 40°S and 50°S; they form near South America and move eastward and poleward where they become quasi-stationary south of Australia [e.g., Mechoso *et al.*, 1991; Harvey *et al.*, 2002]. While inspection of individual days shows many cases where the stratopause is coldest and at lowest altitudes inside the anticyclones, this is not borne out in the multiyear monthly mean maps (we will illustrate this point in section 6). An exception is that the climatological mean stratopause is ~10 K colder inside the anticyclones in September. The geographic pattern in stratopause temperature during this month agrees with Labitzke [1974, Figure 3], who showed radiances at 2 hPa from channel A of the Selective Chopper Radiometer experiment onboard Nimbus 4.

5.3. Winter Synopsis

[33] In order to better understand the mechanism that leads to the zonal asymmetries in the climatological stratopause height and temperature, we now consider the vertical structure of temperature, and how it relates to the vortex and anticyclones. Figure 6 shows the longitude-altitude plots of temperature from 55 to 65°N (45–55°S) for the winter months of DJF (JAS). Figure 6 is analogous to the right column in Figure 2, but for multiyear seasonal averages. Vortex (anticyclone) contours represent 40% and 80% (10% and 50%) of the maximum frequency of occurrence value at each grid point for the season.

[34] In the NH (Figure 6, left), all years are included since the elevated stratopause was confined to higher latitudes (Figure 4j and Randall *et al.* [2009]). In the Arctic during DJF (Figure 6, left), the vortex and anticyclones tilt westward, similar to what is observed in Figure 2 on individual days. At stratopause altitudes (indicated by the gray line),

the temperature is highest inside the vortex. In the anticyclones, the temperature is lower on the eastern flank compared to the western edge. The westward tilted anticyclone and vortex confirms that baroclinic instability is a prevalent condition and associated ageostrophic vertical motions are common. In particular, this results in ascent and cooling on the eastern edge of the anticyclone and descent and warming on the western edge of the anticyclone, leading to anomalies in temperature observed at the stratopause. Similar conditions are observed in the SH during JAS (Figure 6, right); however, the degree to which the circulation systems are vertically tilted as well as the horizontal temperature gradients at the stratopause are both smaller than in the NH.

[35] The baroclinic growth time scale for the Charney model, assuming a vertical wind shear of 60 m/s across the layer 20–50 km, is about 20 days [e.g., Gill, 1982, equation (13.4.3)]. The zonal scale for the linear maximum growth rate is about 6000 km, which is close to wave one at 60° N [Gill, 1982, equation (13.4.4)]. This suggests that transience due to upwelling planetary wave energy from below, which varies on timescales less than 1 week, is probably the dominant process, but baroclinic energy conversion is likely to be important in modulating the process. It is interesting that the planetary wave structure decays above the stratopause, consistent with the reversed temperature gradient, easterly shear, and consequent lack of baroclinic energy conversion. It is also consistent with Rossby wave breaking increasing into the polar mesosphere [Hitchman and Huesmann, 2007].

[36] Figure 7 shows scatterplots of daily mean stratopause temperature and height for the vortex (red) and the anticyclones (black) in the NH during typical DJF seasons (Figure 7, left), in the NH during the two anomalous DJF seasons (Figure 7, middle), and in the SH during JAS (Figure 7, right). The mean and standard deviation of the vortex (anticyclones) stratopause temperature and height are indicated by the blue (gray) dots and bars in order to better quantify the differences between the air masses. These plots

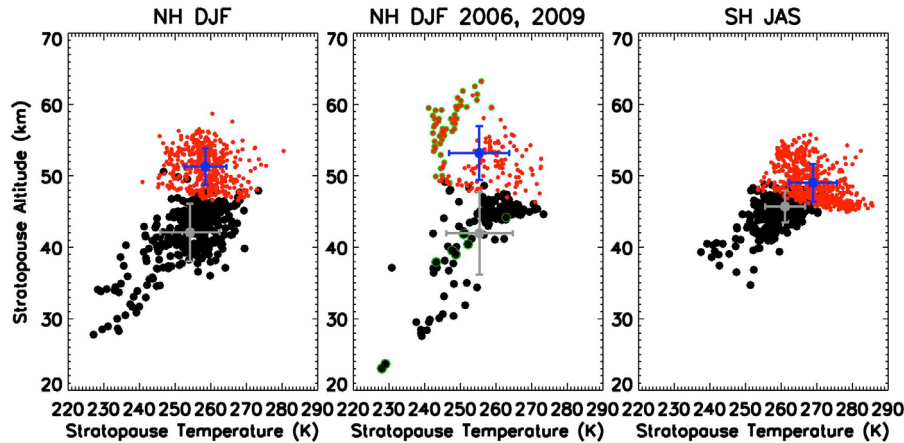


Figure 7. Scatterplots of daily mean stratopause temperature and height in the polar vortex (red) and anticyclones (black) in the (left) NH during typical DJF seasons, (middle) NH during anomalous DJF seasons, and (right) SH during JAS. Figure 7 (left) includes the seasons of 2004/2005, 2006/2007, 2007/2008, 2009/2010, and 2010/2011. Figure 7 (middle) shows the 2005/2006 and 2008/2009 seasons. Green circles in Figure 7 (middle) show February 2006 and 2009. The blue (gray) dots and bars show the mean and one standard deviation of the vortex (anticyclones).

show a distinct difference in the height of the stratopause in the vortex and in the anticyclones. In Figure 7 (left) and Figure 7 (right), the mean height of the stratopause in the Arctic and Antarctic polar vortices is 51 km and 49 km, respectively, and the mean height of the stratopause in the anticyclones is 42 km and 46 km, respectively. The mean temperature of the stratopause in the Arctic and Antarctic vortex is 258 K and 269 K, while the mean temperature in the anticyclones is 254 K and 261 K, respectively. Overall, the stratopause temperature in the polar vortices and anticyclones in both hemispheres displays a large fraction of overlap ($260\text{ K} \pm 5\text{ K}$). In the NH (SH), the daily mean anticyclone stratopause temperature is more than two standard deviations below the mean stratopause temperature in the vortex 20% (17%) of the time. The stratopause height in NH (SH) anticyclones is more than two standard deviations below the mean stratopause height in the vortex 89% (17%) of the time.

[37] For the anomalous seasons of 2005/2006 and 2008/2009 in the NH (Figure 7, middle), the stratopause in the Arctic vortex has a mean height of 53 km and a mean temperature of 255 K, while the anticyclones have a mean height of 42 km and a mean temperature of 255 K. It appears, however, that the vortex means are skewed by the cluster of low-temperature/high-altitude points corresponding to the occurrence of the elevated stratopause during February of these two seasons (indicated by the green circles). If these days are removed from the analysis, the resulting mean stratopause temperature and height in the vortex and anticyclones is 259 K and 52 km, which is within 4 K and 1 km of the mean when these anomalous days are included, indicating that these points have a small affect on the mean of the stratopause height and temperature.

6. Interannual Variability

[38] In order to better understand the statistical significance of the climatology, it is important to quantify the interannual variability of stratopause temperature and height

inside the polar vortices and anticyclones. Figures 8 and 9 show the stratopause temperature (left) and height (right) as a function of time in the vortex (top) and anticyclones (bottom) in the NH (Figure 8) and SH (Figure 9). In both Figures 8 and 9, thin colored lines denote individual years, the thick black line indicates the mean for all years, and the gray shading is one standard deviation from the mean.

6.1. Northern Hemisphere

[39] Figure 8 shows that from late October through January, stratopause temperature in the NH vortex (top left) generally increases by $\sim 15\text{ K}$ and the stratopause descends $\sim 10\text{ km}$ (top right). However, individual years show large ($>5\text{ K}$ and $\sim 3\text{ km}$) fluctuations on weekly timescales. In January and February, there is large ($>10\text{ K}$ and $>10\text{ km}$) interannual variability in both stratopause temperature and height in the vortex. On average the stratopause temperature in the vortex decreases from January to the beginning of March, but in any individual year the temperature variation is much more complex, with 2006 and 2009 showing increases much earlier than the other years. Year 2010 also stands out in that the stratopause temperature in the vortex is higher than in other years in late January but decreases rapidly. Dynamics in 2010 were similar to but not as extraordinary as in 2006 and 2009 [Ayarzagüena *et al.*, 2011]. Mean stratopause height in the vortex increases from January through February, but this increase is largely due to the elevated stratopause events in 2006, 2009, and, to a lesser degree, 2010. The other four years show little change in stratopause height from January through March.

[40] The stratopause temperature and height inside NH anticyclones poleward of 40° N (bottom row) are distinctly different from in the Arctic vortex. The gap in October is a result of a lack of anticyclones poleward of 40° N at the stratopause. From November through May, the stratopause inside the anticyclones is consistently colder and at lower altitudes compared to in the vortex. There is also

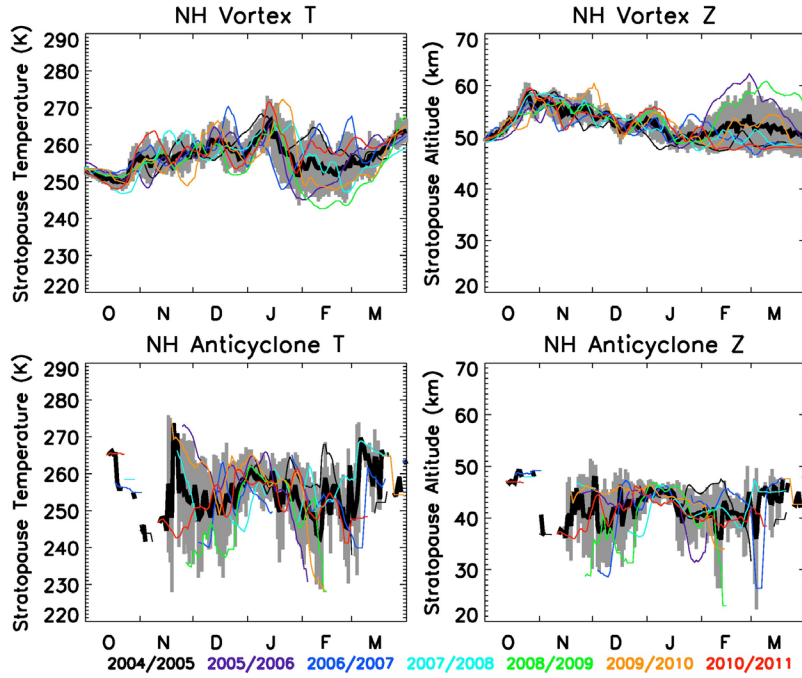


Figure 8. Time series of (left) stratopause temperature and (right) stratopause height inside (top) the Arctic vortex and (bottom) NH anticyclones poleward of 40°N. The thin contours represent a 5-day running mean for each year. Thick black lines represent the daily mean for all years, and the gray shading is the one standard deviation of the annual means.

larger (~ 10 K, ~ 5 km) interannual variability and large variability on daily timescales (as seen by the rapid fluctuations in the colored lines).

[41] The interannual variability of stratopause temperature and height in NH anticyclones is about 10 K and 5 km,

respectively. However, there is a distinct late-December minimum in interannual variability of NH anticyclone stratopause temperature and height. This occurs during a 2 week period in which the vortex stratopause temperature is increasing and the vortex stratopause altitude is decreasing.

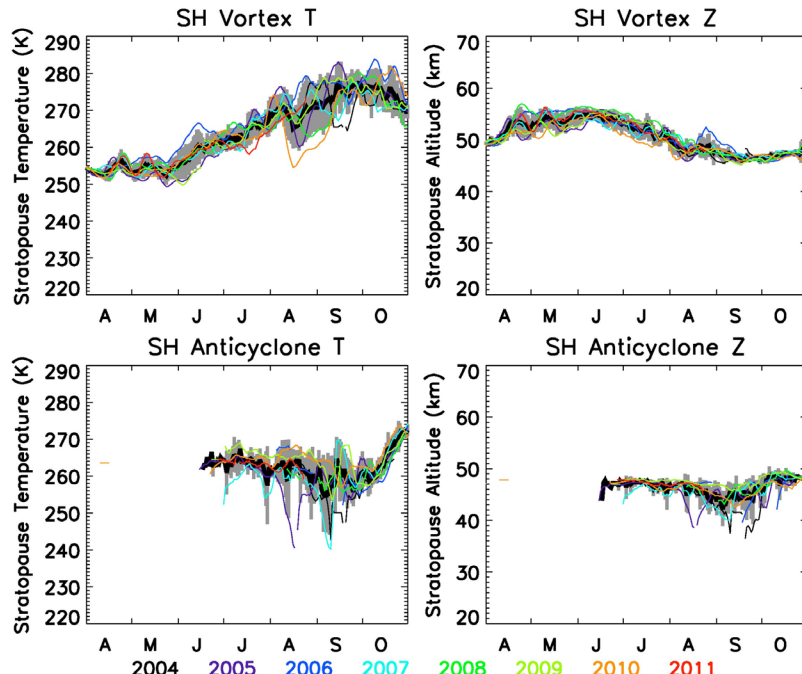


Figure 9. As Figure 8 but for the SH. Anticyclones poleward of 20°S are included.

Investigating the cause of this is beyond the scope of this work.

6.2. Southern Hemisphere

[42] Figure 9 shows the SH time series of stratopause temperature (left column) and height (right column) in the Antarctic vortex (top row) and in SH anticyclones poleward of 20° S (bottom row). In the SH, there is smaller interannual and intraannual variability in stratopause temperature and height in both the vortex and the anticyclones compared to in the NH, as expected. From May through June, GW-driven descent strengthens, causing ~10 K warming of the stratopause in the Antarctic vortex and an elevated stratopause of 55 km in June, when the GW-driven descent is strongest. From July to October, the stratopause gradually descends ~7 km and warms 20 K as GW-driven descent weakens and ozone heating becomes dominant as sunlight returns to the Antarctic.

[43] As in the NH, the stratopause in the SH winter and springtime anticyclones (bottom row) is colder and at lower altitudes compared to the stratopause in the Antarctic vortex. The gap from April to June is a result of a lack of anticyclones poleward of 20°S at the stratopause. There is less interannual and intraannual variability in stratopause temperature and height compared to in the NH, and variability increases somewhat during SH spring, as expected. There are some cases, however, when the daily mean stratopause temperature and height fall below one standard deviation from the 7-year mean. These occur in September 2004, August 2005, and September 2007, following cases of baroclinic instability.

7. Conclusions

[44] In this work we show a 7-year climatology of stratopause temperature and height using MLS data from August 2004 through July 2011 and interpret stratopause temperature and height anomalies with respect to the location of the polar vortices and anticyclones based on GEOS meteorological data. The climatology in the NH is divided into seasons in which there was an elevated stratopause (2005/2006 and 2008/2009) and more typical years (2004/2005, 2006/2007, 2007/2008, 2009/2010, 2010/2011). In the NH winter, planetary-scale anticyclones move eastward and poleward and become stationary near the Aleutian Islands. In the SH spring the anticyclones move rapidly eastward and poleward and become stationary south of Australia. The culmination of repeated synoptic events leads to anomalies in monthly mean stratopause temperature and height. These monthly mean anomalies are most evident in the NH in DJF and in the SH in JAS.

[45] Monthly mean geographic patterns in MLS stratopause temperature and height show that, in both hemispheres, the stratopause is cold and elevated in the vortex during formation. In midwinter, as a result of GW-driven descent, the stratopause is generally elevated and warm in the polar vortices. These results are consistent with the monthly mean zonal mean temperature and zonal wind patterns shown by *Hitchman et al.* [1989]. This work furthers current understanding of the morphology of the stratopause by emphasizing the role of synoptic events in which

anticyclones establish zonally asymmetric climatological patterns in stratopause temperature and height, especially in the NH during DJF and in the SH in JAS.

[46] During the Arctic winter, stratopause temperature is ~20 K lower and stratopause height is 5–10 km lower in the vicinity of the Aleutian anticyclone compared to other longitudes. The geographic distribution of stratopause temperature and height anomalies and their relationship to the climatological positions of the NH anticyclones and the Arctic polar vortex is a direct result of ageostrophic vertical motion resulting from baroclinic instability [*Thayer et al.*, 2010]. Since NH westward tilting anticyclones occur over 60% of the time during these months, baroclinic effects are observed in multiyear monthly means.

[47] During September in the Antarctic, the stratopause is, on average, 10 K colder inside anticyclones south of Australia than outside of the anticyclones. The low stratopause height anomalies observed on daily timescales in the SH spring are obscured from the monthly mean by the rapid poleward and eastward movement of the anticyclones. In the time series, several of these events are indicated by the sharp drop in stratopause height in the anticyclones. The time series also demonstrate that the climatological features discussed in this paper are representative of the individual years, and the interannual variability is small compared with annual variation in the mean, particularly in the vortex.

[48] We show the climatological mean vertical structure of temperature, the polar vortex, anticyclones, and the stratopause near 60° latitude in the NH during DJF and near 50° latitude in the SH during JAS. In both hemispheres, the vortex and anticyclones tilt westward with height, lending further confidence that ageostrophic vertical motions associated with baroclinic instability are common. At stratopause altitudes, low temperatures are associated with local ascent along the eastern edge of the anticyclone. Likewise, high temperatures are observed along the western edge of the anticyclone associated with local descent. In the NH (SH), the daily mean anticyclone stratopause temperature is more than two standard deviations below the mean stratopause temperature in the vortex 20% (17%) of the time. The stratopause height in NH (SH) anticyclones is more than two standard deviations below the mean stratopause height in the vortex 89% (17%) of the time.

[49] The interannual variability in stratopause temperature and height in the polar vortices and anticyclones in both hemispheres is shown. In the Arctic vortex during November and December, individual years show large (>5 K and ~3 km) fluctuations on weekly timescales. In January and February, there is large (>10 K and >10 km) interannual variability in both stratopause temperature and height in the vortex. In NH anticyclones, there is larger (~10 K and ~5 km) interannual variability and larger (>20 K and >10 km) variability on daily timescales. In the SH, there is smaller interannual and intraannual variability in stratopause temperature and height in both the vortex and the anticyclones compared to in the NH, as expected.

[50] Overall, this work emphasizes the need to consider zonal asymmetries in stratopause temperature and height when calculating middle atmosphere temperature trends. Future work will explore whether upper stratospheric

cooling trends are confined to and/or are pronounced in specific geographic regions.

[51] **Acknowledgments.** We thank NASA's GMAO for providing the GEOS analyses and the MLS science team for the processing and distributing the satellite data. We thank Matthias Brakebusch for the MLS gridding routine. Work done at CU was supported by NASA grants NAS5-97046, NNX08AK45G, NNX06AE27G, and NNX10AQ54G, and NSF grants AGS 0940124 and ARC 1107498. M.H.H. was supported by NSF grant ATM 0822858 and NASA grant NNX10AG57G. Research at JPL was supported by NASA.

References

- Ayarzagüena, B., U. Langematz, and E. Serrano (2011), Tropospheric forcing of the stratosphere: A comparative study of the two different major stratospheric warmings in 2009 and 2010, *J. Geophys. Res.*, **116**, D18114, doi:10.1029/2010JD015023.
- Barnett, J. J. (1974), The mean meridional temperature behaviour of the stratosphere from November 1970 to November 1971 derived from measurements by the Selective Chopper Radiometer on Nimbus IV, *Q. J. R. Meteorol. Soc.*, **100**, 505–530, doi:10.1002/qj.49710042602.
- Bloom, S., L. Takacs, A. DaSilva, and D. Ledvina (1996), Data assimilation using incremental analysis updates, *Mon. Weather Rev.*, **124**, 1256–1271, doi:10.1175/1520-0493(1996)124<1256:DAUIAU>2.0.CO;2.
- Charlton-Perez, A. J., L. M. Polvani, J. Austin, and F. Li (2008), The frequency and dynamics of stratospheric sudden warmings in the 21st century, *J. Geophys. Res.*, **113**, D16116, doi:10.1029/2007JD009571.
- Duck, T. J., J. A. Whiteway, and A. I. Carswell (2001), The gravity wave–Arctic stratospheric vortex interaction, *J. Atmos. Sci.*, **58**, 3581–3596, doi:10.1175/1520-0469(2001)058<3581:TGWSAV>2.0.CO;2.
- Fairlie, T. D. A., M. Fisher, and A. O'Neill (1990), The development of narrow baroclinic zones and other small-scale structure in the stratosphere during simulated major warmings, *Q. J. R. Meteorol. Soc.*, **116**, 287–315, doi:10.1002/qj.49711649204.
- Farrara, J. D., M. Fisher, and C. R. Mechoso (1992), Planetary-scale disturbances in the southern stratosphere during early winter, *J. Atmos. Sci.*, **49**, 1757–1775, doi:10.1175/1520-0469(1992)049<1757:PSDTS>2.0.CO;2.
- Garcia, R. R., and B. A. Boville (1994), Downward control of the mean meridional circulation and temperature distribution of the polar winter stratosphere, *J. Atmos. Sci.*, **51**, 2238–2245, doi:10.1175/1520-0469(1994)051<2238:COTMMC>2.0.CO;2.
- Gill, A. E. (1982), *Atmosphere-Ocean Dynamics*, 662 pp., Academic, San Diego, Calif.
- Harvey, V. L., and M. H. Hitchman (1996), A climatology of the Aleutian High, *J. Atmos. Sci.*, **53**, 2088–2102, doi:10.1175/1520-0469(1996)053<2088:ACOTAH>2.0.CO;2.
- Harvey, V. L., et al. (2002), A climatology of stratospheric polar vortices and anticyclones, *J. Geophys. Res.*, **107(D20)**, 4442, doi:10.1029/2001JD001471.
- Hauchecorne, A., et al. (2007), Large increase of NO₂ in the north polar mesosphere in January–February 2004: Evidence of a dynamical origin from GOMOS/ENVISAT and SABER/TIMED data, *Geophys. Res. Lett.*, **34**, L03810, doi:10.1029/2006GL027628.
- Hitchman, M. H., and A. S. Huesmann (2007), A seasonal climatology of Rossby wave breaking in the layer 330–2000 K, *J. Atmos. Sci.*, **64**, 1922–1940, doi:10.1175/JAS3927.1.
- Hitchman, M. H., and C. B. Leovy (1986), Evolution of the zonal mean state in the equatorial middle atmosphere during October 1978 – May 1979, *J. Atmos. Sci.*, **43**, 3159–3176, doi:10.1175/1520-0469(1986)043<3159:EOTZMS>2.0.CO;2.
- Hitchman, M. H., and M. J. Rogal (2010), Influence of tropical convection on the Southern Hemisphere ozone maximum during the winter to spring transition, *J. Geophys. Res.*, **115**, D14118, doi:10.1029/2009JD012883.
- Hitchman, M. H., et al. (1989), The separated polar winter stratopause: A gravity wave driven climatological feature, *J. Atmos. Sci.*, **46**, 410–422, doi:10.1175/1520-0469(1989)046<0410:TSPWSA>2.0.CO;2.
- Holton, J. R. (2004), *An Introduction to Dynamic Meteorology*, 4th ed., 535 pp., Elsevier, San Diego, Calif.
- Hood, L. L. (1986), Coupled stratospheric ozone and temperature response to short-term changes in solar ultraviolet flux: An analysis of Nimbus 7 SBUV and SAMS data, *J. Geophys. Res.*, **91**, 5264–5276, doi:10.1029/JD091iD04p05264.
- Kanzawa, H. (1989), Warm stratopause in the Antarctic winter, *J. Atmos. Sci.*, **46**, 435–438, doi:10.1175/1520-0469(1989)046<0435:WSITAW>2.0.CO;2.
- Labitzke, K. (1974), The temperature in the upper stratosphere: Differences between hemispheres, *J. Geophys. Res.*, **79**, 2171–2175, doi:10.1029/JC079i015p02171.
- Labitzke, K. (1977), Interannual variability of the winter stratosphere in the Northern Hemisphere, *Mon. Weather Rev.*, **105**, 762–770, doi:10.1175/1520-0493(1977)105<0762:IVOTWS>2.0.CO;2.
- Labitzke, K. (1981), Stratospheric-mesospheric midwinter disturbances: A summary of observed characteristics, *J. Geophys. Res.*, **86**, 9665–9678, doi:10.1029/JC086iC10p09665.
- Labitzke, K., and B. Naujokat (2000), The lower Arctic stratosphere in winter since 1952, *SPARC Newslett.*, **15**, 11–14.
- Lahoz, W. A., et al. (1996), Vortex dynamics and the evolution of water vapour in the stratosphere of the southern hemisphere, *Q. J. R. Meteorol. Soc.*, **122**, 423–450, doi:10.1002/qj.49712253007.
- Livesey, N. J., et al. (2011), Earth Observing System (EOS) Microwave Limb Sounder (MLS) Version 3.3 Level 2 data quality and description document, *Rep. JPL D-33509*, Jet Propul. Lab., Pasadena, Calif.
- Manney, G. L., et al. (2008a), The evolution of the stratopause during the 2006 major warming: Satellite data and assimilated meteorological analyses, *J. Geophys. Res.*, **113**, D11115, doi:10.1029/2007JD009097.
- Manney, G. L., et al. (2008b), The high Arctic in extreme winters: Vortex, temperature, and MLS and ACE-FTS trace gas evolution, *Atmos. Chem. Phys.*, **8**, 505–522, doi:10.5194/acp-8-505-2008.
- Manney, G. L., et al. (2009), Aura Microwave Limb Sounder observations of dynamics and transport during the record-breaking 2009 Arctic stratospheric major warming, *Geophys. Res. Lett.*, **36**, L12815, doi:10.1029/2009GL038586.
- Matsuno, T. (1970), Vertical propagation of stationary planetary waves in the winter Northern Hemisphere, *J. Atmos. Sci.*, **27**, 871–883, doi:10.1175/1520-0469(1970)027<0871:VPOSPW>2.0.CO;2.
- McFarlane, N. A. (1987), The effect of orographically excited gravity-wave drag on the general circulation of the lower stratosphere and troposphere, *J. Atmos. Sci.*, **44**, 1775–1800, doi:10.1175/1520-0469(1987)044<1775:TEOOEG>2.0.CO;2.
- Mechoso, C. R., J. D. Farrara, and M. Ghil (1991), Intraseasonal variability of the winter circulation in the Southern Hemisphere atmosphere, *J. Atmos. Sci.*, **48**, 1387–1404, doi:10.1175/1520-0469(1991)048<1387:IVOTWC>2.0.CO;2.
- Meriwether, J. W., and A. J. Gerrard (2004), Mesosphere inversion layers and stratosphere temperature enhancements, *Rev. Geophys.*, **42**, RG3003, doi:10.1029/2003RG000133.
- Mertens, C., et al. (2001), Retrieval of mesospheric and lower thermospheric kinetic temperature from measurements of CO₂ 15 micron Earth limb emission under non-LTE conditions, *Geophys. Res. Lett.*, **28**(7), 1391–1394, doi:10.1029/2000GL012189.
- Olivero, J. J., and G. E. Thomas (2001), Evidence for changes in greenhouse gases in the mesosphere, *Adv. Space Res.*, **28**, 931–936, doi:10.1016/S0273-1177(01)80020-X.
- Pawson, S., et al. (2008), Goddard Earth Observing System chemistry-climate model simulations of stratospheric ozone-temperature coupling between 1950 and 2005, *J. Geophys. Res.*, **113**, D12103, doi:10.1029/2007JD009511.
- Ramaswamy, V., et al. (2001), Stratospheric temperature trends: Observations and model simulations, *Rev. Geophys.*, **39**, 71–122, doi:10.1029/1999RG000065.
- Randall, C. E., V. L. Harvey, D. E. Siskind, J. France, P. F. Bernath, C. D. Boone, and K. A. Walker (2009), NO_x descent in the Arctic middle atmosphere in early 2009, *Geophys. Res. Lett.*, **36**, L18811, doi:10.1029/2009GL039706.
- Rienecker, M. M., et al. (2007), The GEOS Data Assimilation System—Documentation of Versions 5.0.1 and 5.1.0, *Rep. NASA/TM-2007-104606*, 92 pp., NASA Goddard Space Flight Cent., Greenbelt, Md.
- Rind, D., et al. (1998), Climate change and the middle atmosphere. Part III: The doubled CO₂ climate revisited, *J. Clim.*, **11**, 876–894, doi:10.1175/1520-0442(1998)011<0876:CCATMA>2.0.CO;2.
- Russell, J. M., III, M. G. Mlynczak, L. L. Gordley, J. Tansock, and R. Esplin (1999), An overview of the SABER experiment and preliminary calibration results, *Proc. SPIE Int. Soc. Opt. Eng.*, **3756**, 277–288.
- Schwartz, M. J., et al. (2008), Validation of the Aura Microwave Limb Sounder temperature and geopotential height measurements, *J. Geophys. Res.*, **113**, D15S11, doi:10.1029/2007JD008783.
- Simmons, A. J. (1974), Baroclinic instability at the winter stratopause, *Q. J. R. Meteorol. Soc.*, **100**, 531–540, doi:10.1002/qj.49710042603.
- Siskind, D. E., S. D. Eckermann, L. Coy, J. P. McCormack, and C. E. Randall (2007), On recent interannual variability of the Arctic winter mesosphere: Implications for tracer descent, *Geophys. Res. Lett.*, **34**, L09806, doi:10.1029/2007GL029293.

- Thayer, J. P., K. Greer, and V. L. Harvey (2010), Front-like behavior in the Arctic wintertime upper stratosphere and lower mesosphere, *J. Geophys. Res.*, **115**, D00N04, doi:10.1029/2010JD014278.
- Waters, J. W., et al. (2006), The Earth Observing System Microwave Limb Sounder (EOS MLS) on the Aura satellite, *IEEE Trans. Geosci. Remote Sens.*, **44**, 1075–1092, doi:10.1109/TGRS.2006.873771.
- Waugh, D. W., and W. J. Randel (1999), Climatology of Arctic and Antarctic polar vortices using elliptical diagnostics, *J. Atmos. Sci.*, **56**, 1594–1613, doi:10.1175/1520-0469(1999)056<1594:COAAP>2.0.CO;2.
- World Meteorological Organization (1998), SPARC/IOC/GAW assessment of trends in the vertical distribution of ozone, *Global Ozone Res. and Monitor. Proj. Rep.* **43**, Geneva, Switzerland.
-
- J. A. France, V. L. Harvey, and C. E. Randall, Laboratory for Atmospheric and Space Physics, University of Colorado at Boulder, Boulder, CO 80309, USA. (jeffrey.france@colorado.edu)
- M. H. Hitchman, Atmospheric and Oceanic Sciences Department, University of Wisconsin-Madison, Madison, WI 53706, USA.
- M. J. Schwartz, Jet Propulsion Laboratory, 4800 Oak Grove Dr., Pasadena, CA 91109, USA.